



## Modeling and Simulation of a high sensitivity biosensor in a periodic array of metal nanorod pair by using the finite element method

Yuan-Fong Chau, Chien-Ying Chiang, Rong-Moo Hon, Wayne Yang, Li-Chung Wang, Min-Ching Wen, Jia Shiuan Wu and Gung Jing He

Department of Electronic Engineering, Chien Hsin University of Science and Technology  
Zhongli City, Taoyuan County 32097, Taiwan 320, R.O.C.  
yfc01@uch.edu.tw

### ABSTRACT

We numerically investigated the surface plasmon resonances (SPRs) in a periodic array of solid-silver/silver-shell nanorod pair structures for sensing applications by employing a finite-element method. The proposed periodic array of silver-shell nanorod pair structure is composed of a pair of metallic nanorod with a dielectric hole (DH) that interact with a transverse magnetic mode incident plane wave, which includes the investigation of particle–particle interaction. We demonstrate that near-field coupling of the periodic array of solid-silver/silver-shell nanorod pair structures result in a periodic lattice of SPR modes with enhanced field intensities and transmittance dips. The influences of different illumination wavelengths, periods, transmittance spectra, energy flows and electric stream lines, DHs, electric field component distributions and total field intensities, charge density distribution, and the model of the induced local field of the periodic array of solid-silver/silver-shell nanorod pair on “bonding” modes are discussed in our simulations. The proposed structure exhibits a redshifted localized SPR that can be modified over an extended wavelength range of peak resonances and transmittance dips by varying the relative permittivities in DHs and the period of the periodic nanostructure. Simulation results show that the SPR modes are very sensitive to the relative permittivities change in the surrounding materials, which could be used as highly sensitive sensors.

**Keywords:** finite-element method; localized surface Plasmon.

---

# Council for Innovative Research

Peer Review Research Publishing System

**Journal:** Journal of Advances in Mathematics

Vol 5, No. 3

[editor@cirworld.com](mailto:editor@cirworld.com)

[www.cirworld.com](http://www.cirworld.com), [member.cirworld.com](http://member.cirworld.com)



## Introduction

Noble metal nanoparticles (MNPs) (e.g. Au or Ag) that possess a negative real and small positive imaginary dielectric constant are capable of supporting a surface plasmon resonance (SPR) [1-10]. The enhancement in the optical properties of noble MNPs due to the fact that a coherent resonance oscillation of their free electrons in the presence of light, also known as localized surface plasmon resonance (LSPR). LSPR spectroscopy of MNPs is a powerful technique for chemical and biological sensing experiments and biosensing devices. Moreover, the LSPR is responsible for the electromagnetic-field enhancement that leads to surface-enhanced Raman scattering (SERS) and other surface-enhanced spectroscopic processes. The extraordinary transmission of light through nanostructured arrays of subwavelength holes [1] in thin metal films and its relation to SPR [2] has recently inspired researchers to use these devices for label-free biosensing [3].

The diffraction properties of the periodic MNPs allow for light momentum enhancement, thus allowing excitation of SPRs. Such excitation of surface plasmon (SP) waves increases the amount of light scattered inside the dielectric holes (DHs) [11], giving rise to precise peaks in the transmission spectrum at the SPR wavelength. Since the conditions of SPR excitation are extremely sensitive to the refractive medium filled inside the DHs and the surrounding medium, the shift of the peak SPR wavelength is used for real-time detection and studies of biological binding events [6-10].

The capacity to integrate MNPs into biosensing systems has had greatest impact in biology and biomedicine. Metal nanorods are highly suited for SPR sensing [12]. This configuration preserves the collinear geometry that is favored for integration into a suitable SPR device and biosensor. The solid nanorod longitudinal LSPR has considerably higher sensitivity [13] while the metal nanoshell also offers enhanced sensitivity [12]. With decreasing shell thickness (relative to DH size), there is near exponential increase in the plasmon sensitivity [14-16]. Based on this account, we investigate the plasmonic properties of a periodic array of silver (Ag) nanostructures and present the simulation examples of how they are being utilized for biosensing applications. We accentuate in particular how the unique tunability of the SPR properties of MNPs through varying their shape and composition while the MNP size is kept constant. We discuss two interesting nanostructure geometries, including a period array of solid-silver /silver-shell nanorod pairs, that exhibit dramatically enhanced and tunable SPRs, making them highly suitable for biosensing applications. Tuning the MNP shape (e.g., nanorods, or nanoshells) is another means of enhancing the sensitivity of the LSPR to the MNP surrounding and, thereby, designing effective biosensing instrument. Periodic MNP pairs or assemblages display dielectric-dependent SPRs as a result of field coupling. All-inclusive scaling model, relating the SPR frequency to the varying DHs in terms of the varying the MNP size, becomes potentially useful for measuring nanoscale media (and their variations) in biosensing systems.

In the present paper, we numerically investigate the near field intensities and transmittance properties in a periodic array of solid-silver/silver-shell nanorod pair configuration by employing a finite element method (FEM). We demonstrate that near-field coupling of the periodic array of solid-silver/silver-shell nanorod pair structures result in a periodic lattice of SPR modes with enhanced field intensities and transmittance dips. The influences of different illumination wavelengths, periods, transmittance spectra, energy flows and stream lines, DHs, electric field component distributions and total field intensities, charge density distribution, and the model of the induced local field of the periodic array of solid-silver/silver-shell nanorod pair on "bonding" modes are discussed in our simulations. We show that the sensitivities of the periodic array of solid-silver/silver-shell nanorod pair exhibits a linear relationship with DH for the bonding modes in the transmittance spectra. These results suggest alternative schemes to design and improve the sensitivity of plasmon sensor arrays, SERS substrates, plasmonic solar cells, and other nanophotonic devices based on the periodic array of solid-silver/silver-shell nanorod pair structures.

## Simulation Method and Model

The problem of electromagnetic analysis on a macroscopic level is the problem of solving Maxwell's equations subject to certain boundary conditions. The SP's propagation constant can be retrieved by solving Maxwell's equation at the interface of a MNP and a dielectric medium, which yields bonded modes for a transverse magnetic (TM) polarization.

The governing equation can be written in the form

$$\nabla \times (\mu_r^{-1} \nabla \times E) - k_0^2 \epsilon_{rc} E = 0 \quad (1)$$

Where  $\epsilon_{rc}$  is the complex relative permittivity,  $E$  is the electric field intensity,  $k_0$  is the wave vector in free space and  $\mu_r$  is the complex relative permeability.

For the time-harmonic and eigenfrequency problems. The wave number of free space  $k_0$  is defined as

$$k_0 = \omega (\epsilon_0 \mu_0)^{1/2} = \omega / c_0 \quad (2)$$

where  $c_0$  is the speed of light in vacuum and  $\omega$  is the angular frequency. When solving the equations as an eigenfrequency problem the eigenvalue is the complex eigenfrequency  $\lambda = -j\omega + \delta$ , where  $\delta$  is the damping of the solution. Using the relation  $\epsilon_r = n^2$ , where  $n$  is the refractive index, the equation (1) can alternatively be written

$$\nabla \times (\nabla \times E) - k_0^2 n^2 E = 0 \quad (3)$$

When the equation is written using the refractive index, the assumption is that  $\mu_r = 1$  and  $\sigma = 0$  and only the constitutive relations for linear materials are available. When solving for the scattered field the same equations are used but  $E = E_{sc} + E_i$  and  $E_{sc}$  is the dependent variable. In optics and photonics applications, the refractive index is often used instead of the permittivity ( $\epsilon$ ). In materials where  $\mu_r$  is 1, the relation between the complex refractive index,  $n' = n - jk$ , and the complex relative permittivity is  $\epsilon_{rc} = n^2$ , that is  $\epsilon'_r = n'^2 - k^2$ ,  $\epsilon''_r = 2nk$ . The inverse relations are

$$n^2 = 1/2[\epsilon'_r + (\epsilon''_r)^2 + \epsilon''_r]^2] \text{ and } k^2 = 1/2[-\epsilon'_r + (\epsilon''_r)^2 + \epsilon''_r]^2] \quad (4)$$

The parameter  $\kappa$  represents a damping of the electromagnetic wave.

In the approximation that the DHs do not change the dispersion relation of the plasmon, and that there is no strong coupling between the two interfaces of the metallic shell or film, the wavelength that satisfies the condition of SPR excitation of these bonded modes for a diffraction MNP array at normal incident light. We simulate the near-field response and transmittance spectrum of a periodic array of solid-silver/silver-shell nanorod pair structures that interact with a TM incident plane wave by using a FEM, which includes the investigation of MNP–MNP interaction. The enclosure of a pair of silver-shell nanorod with a DH forms an open cavity model, and the electromagnetic field is effectively confined within the gap of the MNP pair to generate high local field enhancement.

The dispersion properties of the MNP must be considered here since the absorption and permittivity of the metallic material are frequency dependent. The Drude-Lorentz dispersion model is used to describe the dependence of the metallic permittivity on the frequency [17], which can be written as

$$\epsilon_0 = \epsilon_\infty + \sum_{j=1}^M (f_j \omega_p^2) / (\omega_{0j}^2 - \omega^2 + i\Gamma_j \omega) \quad (5)$$

where  $\epsilon_\infty$  is the high-frequency contribution to the relative permittivity,  $\omega_p$  is the plasma frequency,  $f_j$  is the oscillator strength,  $\omega_{0j}$  is the resonance frequency, and  $\Gamma_j$  is the damping coefficient.

A FEM that we applied to MNPs was comprehensively described in Refs [18]. We have used the silver permittivity data obtained from Johnson and Christy [19] and corrected with the Drude model, which includes the size effect [20]. In our formulation we used hexahedral high order edge elements. To model an infinite simulation region with a finite-geometry model (i.e., to enclose the computational domain without affecting the numerical solution), it is necessary to use anisotropic perfectly matched layers (PMLs) that are placed before the outer boundary. This formulation can be used to deal with anisotropic material in terms of both dielectric permittivity and magnetic permeability, allowing anisotropic PMLs to be implemented directly.

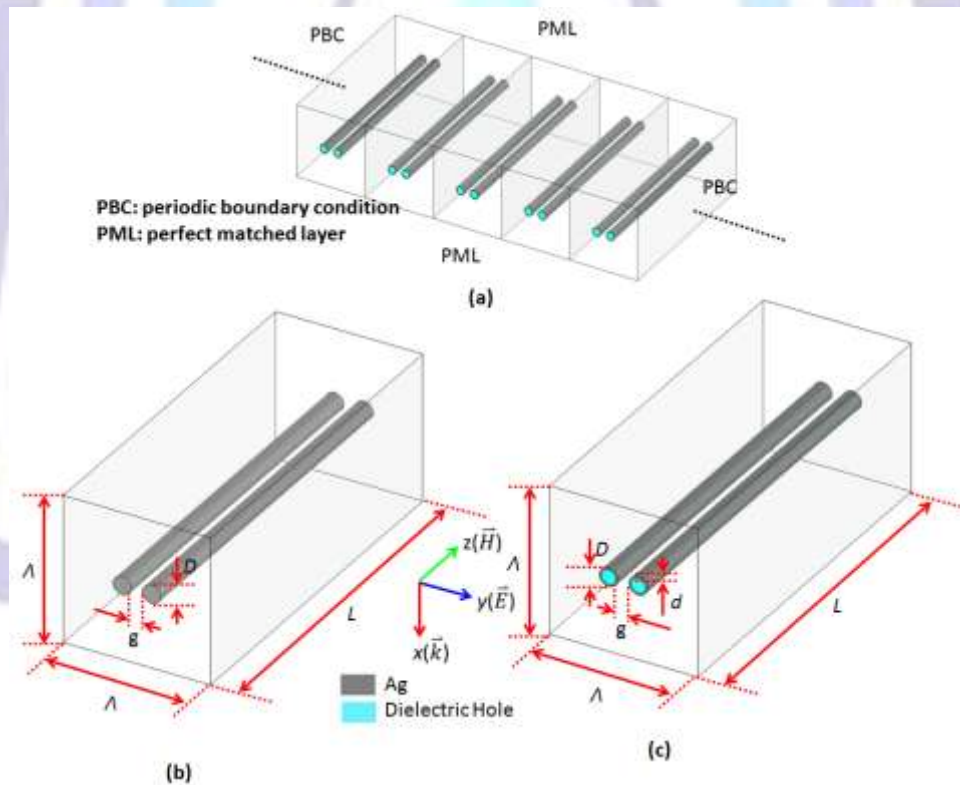


**Fig 1: Schematic plot of simulation models. (a) a period array of grating with solid-silver/silver-shell nanorod pair embedded in the air ( $n=1$ ). (b) a unit cell of solid-silver case, and (c) a unit cell of silver-shell case. All structural parameters are depicted in the inset of this figure.**

Figure 1 shows the considered grating, with a period array of solid-silver/silver-shell nanorod pair embedded in the air ( $n=1$ ). The grating period, or the distance between the nanorods, is  $\Lambda$ . According to our previous work [11], the structural parameters are set as: diameter of each nanorod  $D=50$  nm, shell thickness  $d=10$  nm and the nanorod pair separated by a gap  $g=20$  nm. The DH can be filled with different relative permittivities (i.e.,  $\epsilon=1, 3, 5, 8$  and  $10$ ) of media inside the silver-shell nanorods. The amplitude of the incident light is set to be 1 V/m throughout this paper. The near-field intensity measured the middle point in the gap region.

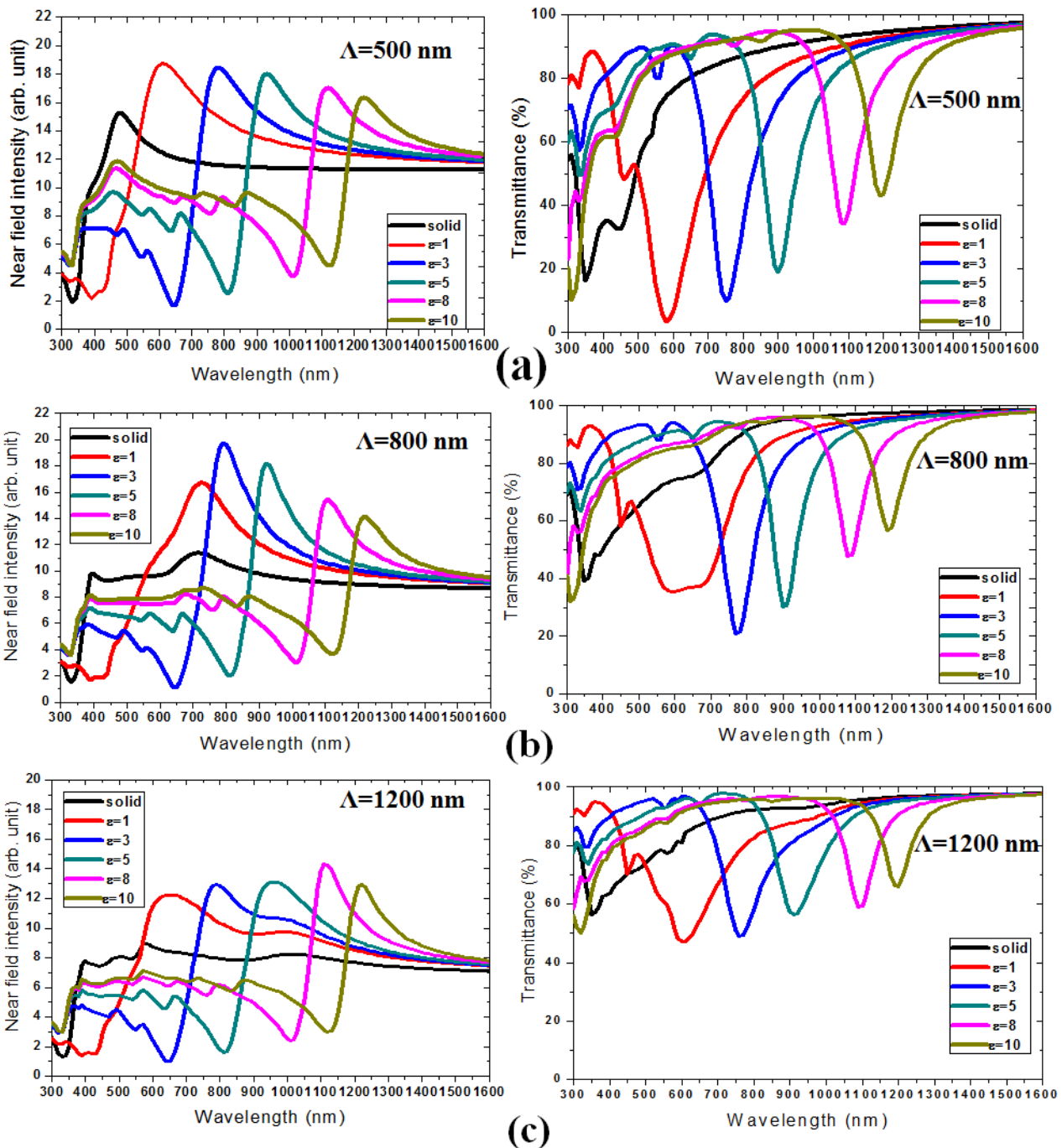


**Fig 2: Near field intensities (left side) and transmittance (right side) vs. wavelengths as the period expands from (a) 500 nm, (b) 800 nm to (c) 1200 nm.**

### Optimization, Results and discussion

Periodic MNPs are often more interesting than single structure because of the strong coupling effects. One way of tuning the LSPR is by changing the MNP shape from spherical to rod-shaped. Rod-shaped MNPs have two resonances: one owing to SP oscillation along the nanorod short axis and another due to SP oscillation along the long axis [4,5,12]. The second method of LSPR tuning is by using a metal nanoshell [21]. Starting from a solid spherical MNP, as one decrease shell thickness, the LSPR red-shifts from the visible to the NIR [8,21] due to increased coupling between the inner and outer shell SPs [12,22,23]. The period  $\Delta$  denotes the density of the periodic silver-shell nanorod arrays in the fabrication process. The period ( $\Delta$ ) of nanorod pair represents an essential feature like the other MNPs. Figures 2(a)-2(c) show the near field intensities (left side) and transmittance (right side) vs. wavelengths as the period expands from 500 nm to 1200 nm. For the near-field intensities as shown in the left side of Figs. 2(a)-2(c), one can see that the near field intensities can be enhanced as the decreasing period ( $\Delta$ ) and the red-shift can be achieved as the relative permittivity filled inside the DHs is increased.

The right side of Figs. 2(a)-(c) shows the transmittance spectra of solid-silver nanorod (solid case, black line) and silver-shell nanorod (DH cases) with five different relative permittivities (i.e.,  $\epsilon = 1, 3, 5, 8$  and  $10$ ) filled inside the DHs. The transmittance dips for smaller periods (e.g.,  $\Lambda=500$  nm) are much deeper than that of larger ones (e.g.,  $\Lambda=1200$  nm), and red-shift toward higher wavelengths. It is evident that the transmittance dip and the red-shifted can be easily tuned by varying the filling relative permittivity filled inside the DHs and the length of the nanorod pair array period ( $\Lambda$ ).

The same trend of transmittance resonance dip wavelength (TRDW) can be also found in the right side of Figs. 2(a)-2(c). In the right side of Figs. 2(a)-2(c), the appearance of TRDW is due to the SP excitation [24, 25]. The following equation is the excitation condition,

$$k_0[(\epsilon_n \epsilon_{Ag} / \epsilon_n) + \epsilon_{Ag}] = 2\pi N / \Lambda \quad (6)$$

where  $N$  is an integer,  $k_0$  is the vacuum wave vector,  $\Lambda$  is the period, and  $\epsilon_{Ag}$  and  $\epsilon_n$  are the dielectric constant of silver and adjacent dielectric, respectively. According to Eq. (6), the SPR is mainly governed by the period ( $\Lambda$ ). However, the TRDW of silver-shell nanorod case is caused by F-P like resonance due to the gap between the nanorod pair and hollow region in DH. It has been proved that when incident light impinges on the surface of the nanorod pair, localized SPRs are excited and pass through the gap and hollow regions (DHs), and the F-P like resonance in the gap and hollow regions leads to the electric field enhancement and transmittance dips [26,27].

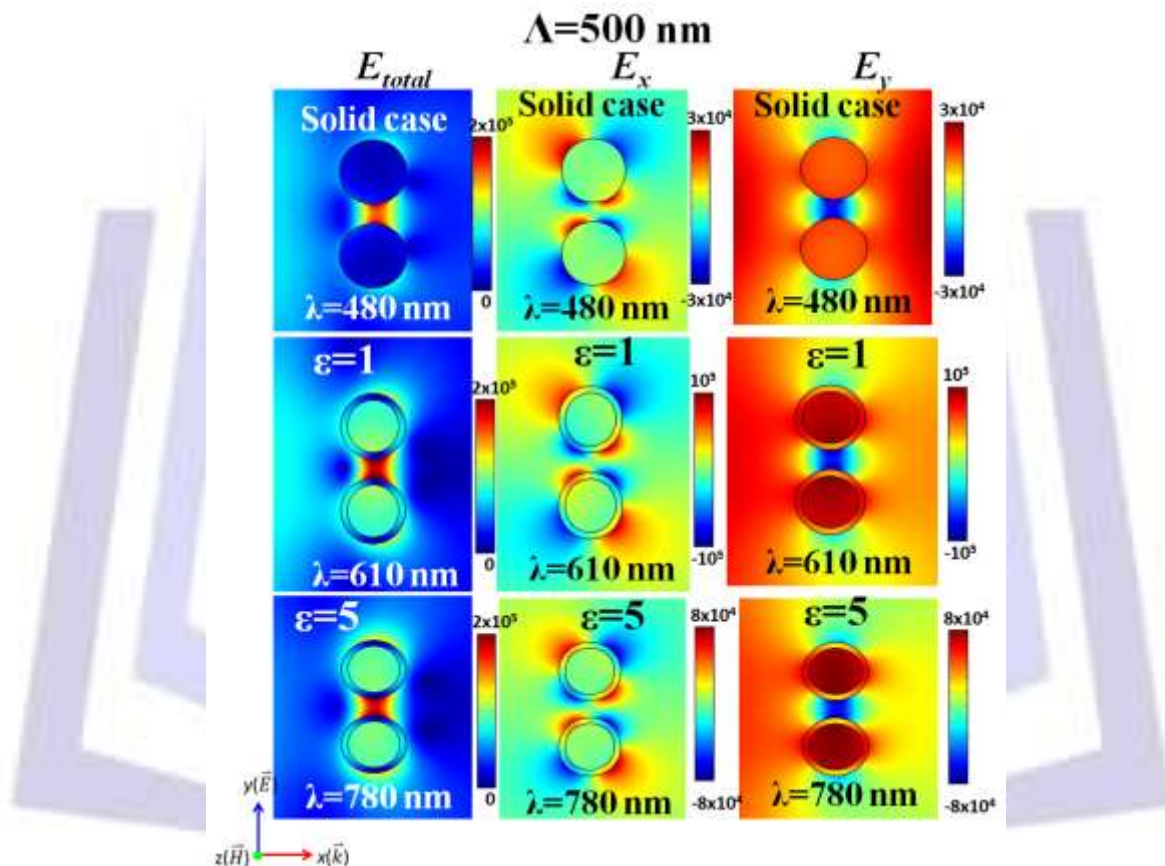


**Fig 3: Corresponding SPR modes of near-field distributions of no DH (i.e., solid case, see the first row) and DH cases (see the 2nd-3th rows) with shell thickness  $d = 10$  nm and period  $\Lambda = 500$  nm and different relative permittivities filled inside the DHs.**

For these media filled inside the DHs, we show how the periodic array of solid-silver/silver-shell nanorod structures resonances are varied with the DH medium and period while the overall particle size and aspect ratio of the MNP are held constant. As the DH relative permittivity decreased (e.g.,  $\epsilon = 1$  and  $3$ ), the hybridization between the DHs and spheroid modes becomes progressively stronger, resulting in larger energy gaps between the bonding and anti-bonding plasmon modes [24,25]. The “bonding” SP modes of the proposed silver-shell nanorod structures occurred at the transmittance dips (see the right sides of Figs. 2(a)-2(c)) are more sensitive to the relative permittivity filled inside the DH than the solid-silver case. The silver-shell nanorod SP modes have a significantly increased the geometrically and materially sensitive hybrid SPRs by varying the relative permittivity filled inside the DH and can be tuned across a broader spectral range than the modes of solid-silver case. Near-field intensity and transmittance spectra can be tuned by varying relative permittivity filled inside the DH of the silver-shell nanorod arrays. Such environmental sensitivity of the plasmons of silver-shell nanorod holds great potential for monitoring local environmental changes during chemical, biological processes, switchable plasmonic devices, and plasmonic solar cell. For example, it is possible to tune and shift the optical responses of the silver-shell nanorods system by filling “phase change materials” (dielectric constant can be switchable through

modulation of the input energy for phase transition between amorphous and crystalline phase states [28-30] ) inside the silver-shell nanorods.

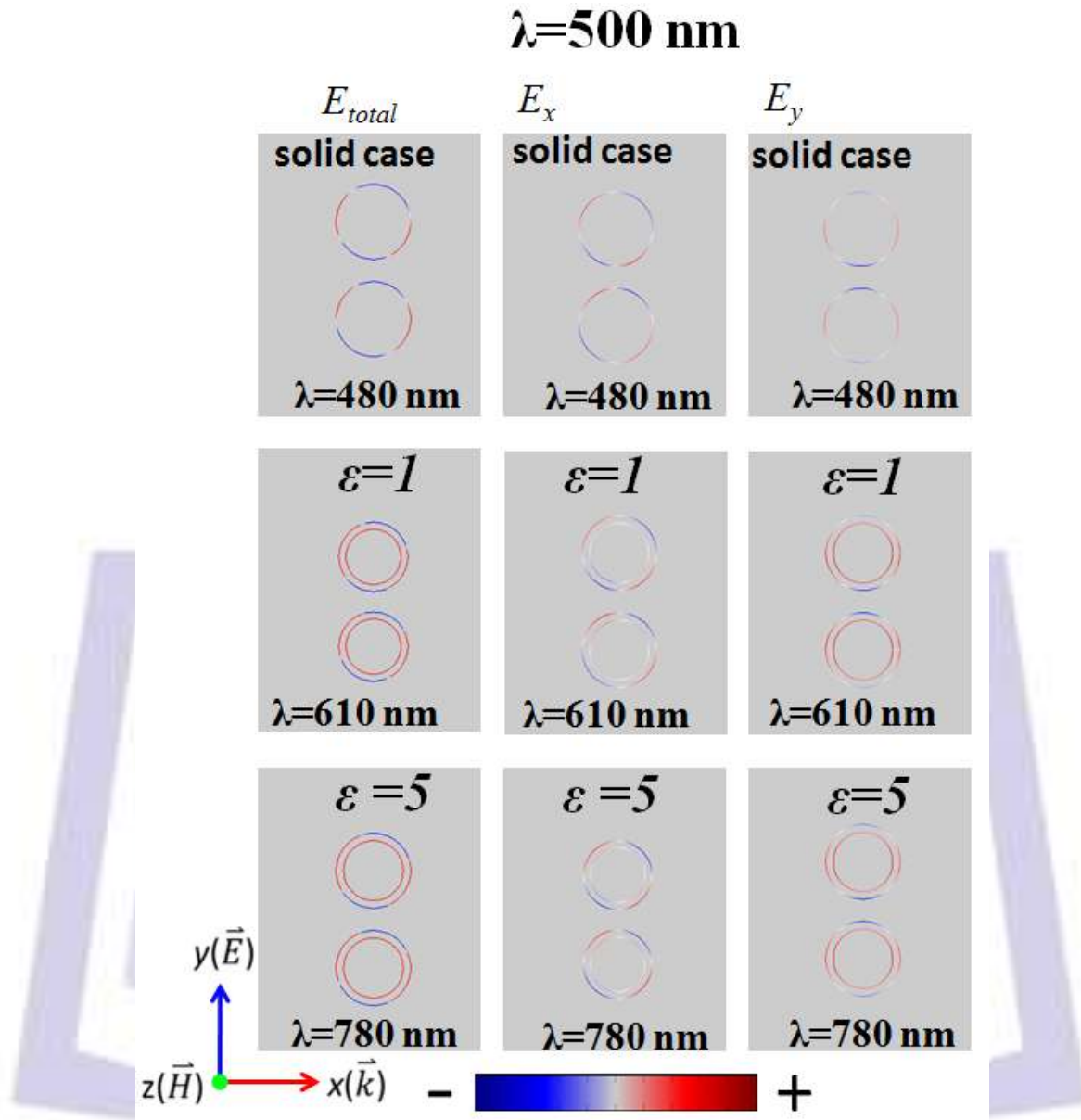


**Fig 4: Corresponding SPR modes of charge distributions of solid case (see the first row) and DH cases (see the 2nd-3th rows) with shell thickness  $d = 10$  nm and period  $\lambda = 500$  nm and different relative permittivities filled inside the DHs.**

In order to realize the detailed behaviors of the field distribution inside the system consisting of a periodic array of solid-silver/silver-shell nanorod structures with different DHs, the electric field component distributions and total field intensity will be discussed here. To find the contribution of SPRs, we plot the selected polarization components of the electric field distribution, i.e., the TM mode near-field distributions of two components  $E_x$  and  $E_y$ , and total field intensity distribution  $E_{total}$ .

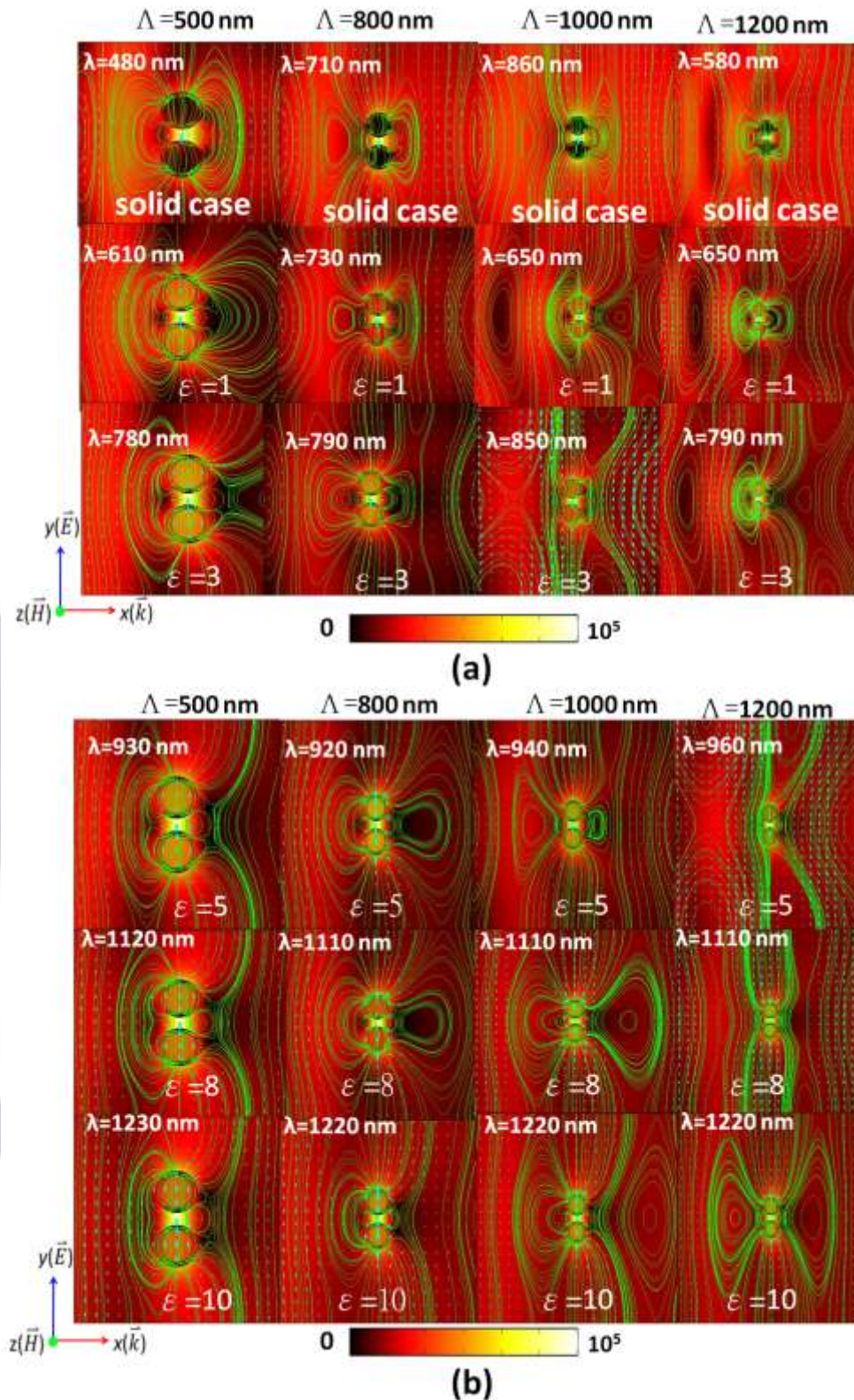


**Fig 5: Schematic plot of corresponding SPR modes, energy flows and electric field stream lines. (a) for solid case,  $\epsilon=1$ , and  $\epsilon=3$ , and (b) for  $\epsilon=5$ , 8 and 10, respectively.**

Figure 3 illustrates the near-field distributions of solid case (see the first row) and DH cases (see the 2<sup>nd</sup>-3<sup>rd</sup> rows) with different relative permittivities (i.e.,  $\epsilon = 1$  and  $5$ , respectively) filled inside the DHs. The other parameters, shell thickness  $d$  and period ( $\Lambda$ ), are set to be  $d=10$  nm and  $\Lambda = 500$  nm, respectively. From the results revealed in Fig. 3, we find that SPs can be excited surrounding the surfaces and rims of the solid-silver/silver-shell nanorod pair structure. The x-component of the electric field  $E_x$  shows eight distinct petals of distribution around the solid-silver/silver-shell nanorod showing no field distributions inside the DHs. The y-component of the electric field  $E_y$  is distributed symmetrically along the side surface of



the solid-silver/silver-shell nanorod showing four petals of distribution. As can be seen in the left side of Fig. 3, the total field intensities  $E_{total}$  at their corresponding SPR wavelengths (i.e.,  $\lambda=610$  nm and  $\lambda=780$  nm) show a hybridized plasmon mode on the inner and the outer silver-shell surfaces, namely, the hybridization of the void plasmon and the associated liner SP. The strongest field intensity (peak value) is found in the gap of the solid-silver/silver-shell nanorod pair. Note that the localized electric field enhancement at the circumference of the solid-silver/silver-shell nanorod extends in the tens of nanometers range from their surface.

Regarding the direction of electric field distributions as shown in Figs. 3, the schematic charge densities of the selected cases in Fig. 3 are also depicted in Fig. 4, respectively. It can be seen that the charge density on the outer surfaces of the solid cases (see the first row of Fig. 4) is arranged in the form of one layer distribution. Turning to the DH cases (see the 2<sup>nd</sup> and 3<sup>rd</sup> rows of Fig. 4), the charge densities on the inner and outer surfaces of silver-shell are arranged in the form of two layers distribution and exhibit stronger dipole-like interactions than that of solid case, leading to a bonding mode resonance.

In order to realize the mechanism on above-mentioned phenomena, the selected near field distributions for the cases of solid-silver/silver-shell nanorod pair structure with different periods (i.e.,  $\Lambda=500, 800, 1000$  and  $1200$  nm), and the varying DHs (i.e.,  $\epsilon=1, 3, 5, 8$  and  $10$ ) and their corresponding SPR modes, energy flows and electric field stream lines are also depicted in Figs. 5(a) and 5(b), respectively. Because of coupling effects between a pair of silver-shell nanorod, we find that the electric field is enhanced and forms a hot spot in the gap, and the electric field is suppressed elsewhere, which shows quite different pattern from the results obtained from a single silver nanorod arrays (results not shown here).

Due to the intensive localization of electromagnetic energy inside the proposed structures, the SPR wavelengths of the electric field SP modes were very sensitive to the relative permittivities changed in the surrounding materials. Thus, the periodic array of the solid-silver/silver-shell nanorod pair structures could be used as highly sensitive sensors. As discussed in Fig. 2, an intriguing feature of the SP oscillation is that its SPR wavelength depends on the dielectric media filled inside the hollow region [10,12-14]. With increase in refractive permittivity, the LSPR red-shifts. When this shift is followed using scattering spectroscopy (for MNPs deposited on a substrate) or absorption spectroscopy (for colloidal MNPs), changes in the MNP surroundings can be sensed [12].

## Conclusion

In conclusion, we numerically investigated the sensing properties of the electric SPR modes of the periodic array of the solid-silver/silver-shell nanorod pair structures which are composed of a metallic nanorod pairs and DHs by using of the finite-element method. We show how the periodic array of solid-silver/silver-shell nanorod pair structures resonances are varied with the DH medium and period of nanostructure while the overall particle size and aspect ratio of the MNP are held constant. The near-field distribution is strongly confined within the proposed structures at the SPR modes, leading to greater field-material interactions and increased sensitivity to the relative permittivity changes in DHs. The proposed periodic composited nanostructures retain the collinear geometry that is favored for integration into a suitable SPR device and are sufficient for single molecule detection and other applications in biosensors.

## Acknowledgment

The author acknowledges the financial support from the National Science Council of the Republic of China (Taiwan) under Contract No. NSC 102-2112-M-231-001-.

## References

- [1] T. W. Ebbesen, H. J. Lezec, H. F. Ghaemi, T. Thio, and P. A., "Wolff Extraordinary optical transmission through sub-wavelength hole arrays," *Nature* 391, 667–669 (1998).
- [2] H. F. Ghaemi, T. Thio, D. E. Grupp, T. W. Ebbesen, and H. J. Lezec, "Surface plasmons enhance optical transmission through subwavelength holes," *Phys. Rev. B* 58, 6779–6782 (1998).
- [3] A. G. Brolo, R. Gordon, B. Leathem, and K. L. Kavanagh, "Surface plasmon sensor based on the enhanced light transmission through arrays of nanoholes in gold films," *Langmuir* 20, 4813–4815 (2004).
- [4] Murphy, C. J.; Sau, T. K.; Gole, A. M.; Orendorff, C. J.; Gao, J.; Gou, L.; Hunyadi, S. E.; Li, T., "Anisotropic Metal Nanoparticles, Synthesis, Assembly, and Optical Applications," *J. Phys. Chem. B*, 109, 13857–13870 (2005).
- [5] Link, S.; Mohamed, M. B.; El-Sayed, M. A. Simulation of the Optical Absorption Spectra of Gold Nanorods as a Function of Their Aspect Ratio and the Effect of the Medium Dielectric Constant. *J. Phys. Chem. B* 1999, 103, 3073–3077. Erratum: *J. Phys. Chem. B* 2005, 109, 10531-10532.
- [6] Jana, N. R.; Gearheart, L.; Murphy, C. J. Seed-Mediated Growth Approach for Shape-Controlled Synthesis of Spheroidal and Rod-like Gold Nanoparticles Using a Surfactant Template. *Adv. Mater.* 2001, 13, 1389–1393.
- [7] Nikoobakht, B.; El-Sayed, M. A. Preparation and Growth Mechanism of Gold Nanorods (NRs) Using Seed-Mediated Growth Method. *Chem. Mater.* 2003, 15, 1957–1962.
- [8] Jain, P. K.; El-Sayed, M. A. Universal Scaling of Plasmon Coupling in Metal Nanostructures: Extension from Particle Pairs to Nanoshells. *Nano Lett.* 2007, 7, 2854–2858.



- [9] Prodan, E.; Radloff, C.; Halas, N. J.; Nordlander, P. A Hybridization Model for the Plasmon Response of Complex Nanostructures. *Science* 2003, 302, 419–422.
- [10] Haes, A. J.; Van Duyne, R. P. A Nanoscale Optical Biosensor: Sensitivity and Selectivity of an Approach Based on the Localized Surface Plasmon Resonance Spectroscopy of Triangular Silver Nanoparticles. *J. Am. Chem. Soc.* 2002, 124, 10596–10604.
- [11] Yuan-Fong Chau, "Surface Plasmon Effects Excited by the Dielectric Hole in a Silver-Shell Nanospherical Pair," *Plasmonics* 4:253–259 (2009).
- [12] Prashant K. Jain, Xiaohu Huang, Ivan H. El-Sayed, and Mostafa A. El-Sayed, "Noble Metals on the Nanoscale: Optical and Photothermal Properties and Some Applications in Imaging, Sensing, Biology, and Medicine," *Accounts of Chemical Research*, 41, 1578-1586 (2008)
- [13] Lee, K.-S.; El-Sayed, M. A. Gold and Silver Nanoparticles in Sensing and Imaging: Sensitivity of Plasmon Response to Size, Shape, and Metal Composition. *J. Phys. Chem. B* 110, 19220–19225 (200).
- [14] Underwood, S.; Mulvaney, P. Effect of the Solution Refractive Index on the Color of Gold Colloids. *Langmuir* 1994, 10, 3427–3430.
- [15] Haes, A. J.; Zou, S.; Schatz, G. C.; Van Duyne, R. P. Nanoscale Optical Biosensor: Short Range Distance Dependence of the Localized Surface Plasmon Resonance of Noble Metal Nanoparticles. *J. Phys. Chem. B* 108, 6961–6968 (2004).
- [16] Jain, P. K.; El-Sayed, M. A. Surface Plasmon Resonance Sensitivity of Metal Nanostructures: Physical Basis and Universal Scaling in Metal Nanoshells. *J. Phys. Chem. C* 111, 17451–17454 (2007).
- [17] Bohren CF, Huffman DR (1983) *Absorption and Scattering of Light by Small Particles*, Wiley.
- [18] Jin J (2002) *The Finite Element Method in Electrodynamics* (Wiley).
- [19] Johnson PB, Christy RW (1972) Optical constants of the noble metals. *Phys. Rev. B* 6: 4370–4379
- [20] M. Young, *The Technical Writer's Handbook*. Mill Valley, CA: University Science, 1989.
- [21] Oldenburg, S. J.; Averitt, R. D.; Westcott, S. L.; Halas, N. J. Nanoengineering of Optical Resonances. *Chem. Phys. Lett.* 1998, 28, 243–24.
- [22] El-Sayed, I. H.; Huang, X.; El-Sayed, M. A. Surface Plasmon Resonance Scattering and Absorption of Anti-EGFR Antibody Conjugated Gold Nanoparticles in Cancer Diagnostics: Applications in Oral Cancer. *Nano Lett.* 2005, 5, 829–834.
- [23] Alivisatos, A. P. The Use of Nanocrystals in Biological Detection. *Nat. Biotechnol.* 2004, 22, 47–52.
- [24] S. Aksu, A. A. Yanik, R. Adato, A. Artar, M. Huang, and H. Altug (2010) High-Throughput Nanofabrication of Infrared Plasmonic Nanoantenna Arrays for Vibrational Nanospectroscopy. *Nano. Lett.* 10: 2511-2518
- [25] Y.-F. Chau, H.-H. Yeh, and D. P. Tsai (2008) Near-field optical properties and surface plasmon effects generated by a dielectric hole in a silver-shell nanocylinder pair. *Appl. Opt.* 47: 5557-5561.
- [26] F, Nehl CL, Hafner JH, Nordlander P (2007) Plasmon resonances of a gold nanostar. *Nano Lett* 7:729–732
- [27] Hao F, Sonnefraud Y, Dorpe PV, Maier SA, Halas NJ, Nordlander P (2008) Symmetry breaking in plasmonic nanocavities: subradiant LSPR sensing and tunable Fano resonance. *Nano Lett* 8:3983–3988
- [28] Aizpurua J, Hanar P, Sutherland DS, Kall M, Bryant GW, de Garc'ia FJAbajo (2003) Optical properties of gold nanorings. *Phys Rev Lett* 90:057401.
- [29] Samson ZL, MacDonald KF, De Angelis F, Gholipour B, Knight K, Huang CC, Di Fabrizio E, Hewak DW, Zheludev NI (2010) Metamaterial electro-optic switch of nanoscale thickness. *Appl Phys Lett* 96:143105.
- [30] Tseng ML, Chen BH, Chu CH, Chang CM, Lin WC, Chu NN, Mansuripur M, Liu AQ, Tsai DP (2011) Fabrication of phase-change chalcogenide Ge<sub>2</sub>Sb<sub>2</sub>Te<sub>5</sub> patterns by laser-induced forward transfer. *Opt Express* 19:16975.